ChemComm

Accepted Manuscript

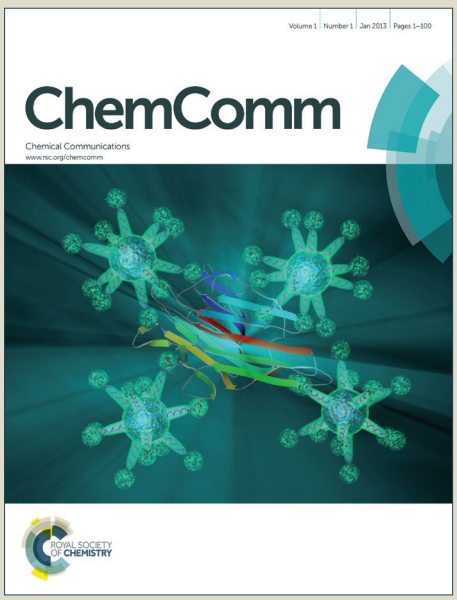

ROYAL SOCIETY OF CHEMISTRY

www.rsc.org/chemcomm

Kinetic and Thermodynamic Processes of Organic Species at the Solution Solid Interface: The view through an STM.

Ursula Mazur and K W Hipps*

Chemistry Department and Materials Science and Engineering Program

Washington State University, Pullman, WA 99164-4630

hipps@wsu.edu

ABSTRACT: A focused review is presented on the evolution of our understanding of the kinetic and thermodynamic factors that play a critical role in the formation of well ordered organic adlayers at the solution-solid interface. While the current state of knowledge is in the very early stages, it is now clear that assumptions of kinetic or thermodynamic control are dangerous and require careful confirmation. Equilibrium processes at the solution-solid interface are being described by evolving thermodynamic models that utilize concepts from the thermodynamics of micelles. A surface adsorption version of the Born-Haber cycle is helping to extract the thermodynamic functions of state associated with equilibrium structures, but only a very few systems have been so analyzed. The kinetics of surface phase transformation, especially for polymorphic phases is in an early qualitative stage. Adsorption and desorption kinetics are just starting to be measured. The study of kinetics and thermodynamics for organic self-assembly at the solution-solid interface is experiencing very exciting and rapid growth.

Introduction

Understanding and predicting the chemistry that occurs at the solution-solid interface is of critical importance for a wide range of modern scientific and technological problems. Molecular self-assembly from solution onto surfaces is widely embraced as a strategy for creating adlayers with desirable electronic, photonic, and chemical properties. Catalysis and battery development also are intimately dependent on the chemistry that occurs at the solution solid interface. If we are to develop a rational method for predicting the surface structures that yield optimal processes, we must understand the fundamentals about how adlayers are formed and react at the solution-solid interface. This great importance is counter balanced by a very limited selection of tools for studying this interface at the molecular – or even sub molecular – level. Scanning probe microscopy, and especially scanning tunneling microscopy (STM) offers the ability to perform these studies in various solution environments, at varying temperature and pressure, and with changing solute composition. Thus, STM has become the primary tool for analyzing structure,

monitoring the time dependence of processes, and extracting thermodynamic data from systems where the critical action occurs at the nanoscale.[1-6] To date, most variable temperature and composition STM studies at the solid-solution interface have been performed with home made or commercial instruments using heated (only) samples.[7-9] Very recently an alternative configuration wherein the entire STM exists in a controlled environment has been demonstrated.[10]

Throughout the last two centuries, understanding chemical reactions has included the ability to measure kinetics (rates of reaction) and to measure and/or predict the thermodynamically stable product. This competition between kinetics and thermodynamics is a fundamental conflict that underlies all of chemistry. Thus, a qualitative and quantitative understanding of the kinetics and thermodynamics that occur at the solution-solid interface is an essential component to achieving the desirable goal of predicting surface structures and their chemical and electronic properties. Unfortunately, there is very little known quantitatively about kinetics and thermodynamics at the solution-solid interface, and only somewhat more is know qualitatively. Thus, an important and rapidly advancing frontier is the quantitative understanding of the relative roles of kinetics and thermodynamics at the solid solution interface.

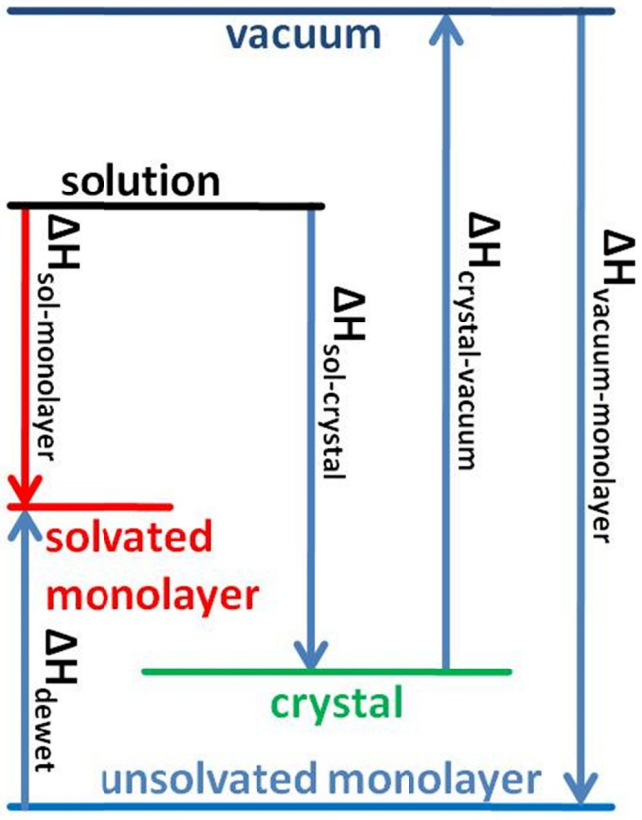

Figure 1: Born-Haber cycle diagram. Reprinted with permission from reference 11. Copyright 2013 American Chemical Society.

On the laboratory scale, the variables of special interest are temperature, concentration, solvent, pressure, and time. On the molecular scale the issues of interest include structure, polymorphism, location of processes (on terraces, at boundaries or defects, within islands, etc.), residence time at a particular site, and solvent co-adsorption. A highly desirable goal is to measure a surface process with respect to all these variables

and thereby determine all the rate constants and thermodynamic variables associated with each step in the process. To achieve this, we need detailed knowledge of the solvation of the solute, the solvation of the surface, the solute-solute interactions (both in solution and on the surface), solute-surface interaction, solvent-surface (with both the substrate and the newly formed adlayer), and the role of any inhomogeneities on the surface such as defects, step edges, or reconstructions. An approximate graphical presentation of the thermodynamic relationships (for the case of the enthalpy) was given by Lackinger [11] and is reproduced with his permission as Figure 1. Of course, this diagram works equally well for any function of state.

In order to specify kinetics, we need the rates of adsorption, the nucleation rate, the growth rate, the diffusion rate on the surface, the desorption rates (from different sites), the diffusion rate from solution to the surface, and the desorption rate for the solvent (both from the substrate and the adlayer). For no system do we currently have all of these parameters. In fact, for very few systems do we even know if the structure observed is in dynamic equilibrium with the solvent.

The temperature dependence of rate constants is generally treated in one of two ways.[12] The Arrhenius equation, $k = k_0 e^{-\frac{\Delta E}{RT}}$, assumes an activation energy ΔE that must be thermally surmounted and k_0 is interpreted as an attempt frequency, generally of the order of 10^{12} Hz to 10^{14} Hz. Alternatively, the rate constant can be expressed in terms of the Eyring transition state theory to be $k = \frac{k_B T}{h} e^{\frac{\Delta S^+}{R}} e^{-\frac{\Delta H^+}{RT}}$ where ΔH^+ and ΔS^+ are enthalpy and entropy associated with formation of the activated complex. The first of three terms is 6.6×10^{12} Hz at 293 K, making the two different formulations numerically similar when the entropy of activation is small, but quite different when there is a large difference in entropy (as in desorption from the surface).

Thermal Annealing

The simplest type of experiment that can produce qualitative information about the roles of thermodynamics and kinetics at the solution-solid interface is thermal annealing, where a sample is heated for a fixed period and then allowed to cool to room temperature for measurement. We used this method to investigate the adsorption of coronene on Au(111) from an alkanoic acid solution.[13] We were able to show that the neither the dense packed nor more open polymorphs seen at room temperature were stable above about 100ºC but that the rate of desorption was such that it required several minutes to significantly remove coronene from the surface. These annealing experiments also demonstrated that solvent co-adsorption was an important factor in

the thermal stability. In addition, the high temperature desorption was initiated at defects and grain boundaries and then grew from there in a manner similar to a grass fire. Thus, kinetics played a significant role in the desorption process.

Marie and co workers studied the role of annealing (up to 50ºC) on hexakis(n-dodecyl)-peri-hexabenzocoronene (HBC-C12) adsorption on Au(111) from an n-tetradecane solution.[14] They demonstrated that the packing density of the HBC-C12 could be tuned with annealing temperature as the adlayer underwent three different phase transitions over that temperature range. STM images revealed that the packing density increase is the result of stepwise desorption of n-dodecyl chains allowing the HBC cores to occupy more of the surface. The three transitions were all irreversible leaving an open question as to whether they were entirely kinetically controlled, or if the last one was the equilibrium (thermodynamic) state. De Feyter and coworkers observed similar phenomena (tuning packing density by annealing) in the case of lead pyrenocyanine at the phenyloctane/HOPG interface. [15] Annealing at 60°C resulted in a transition to a new phase that remained stable upon cooling. Thus, it is likely that the room temperature structure is kinetically controlled.

A very recent example of the use of thermal annealing to interrogate the role of kinetics and thermodynamics in the development of a particular surface structure was presented by Hu and coworkers.[16] They investigated the self assembly of phthalocyanine arrays using triphenylene-2,6,10-tricarboxylic acid as a nanotemplate. The solvent used was 1-heptanoic acid and the substrate was HOPG. By a combination of concentration and temperature tuning, they were able to observe five different arrays, including one thermodynamically stable form. The thermodynamically stable structure achieved by annealing at 323 K for 10 minutes had very large grains and few defects.

While none of these studies give quantitative insights into the rates of critical processes or values for enthalpies or entropies associated with the thermodynamically stable forms, they do clearly show that kinetics is often more important than thermodynamics for adlayers formed near room temperature at the solution solid interface. We next turn our attention to actual measurement or calculations of critical thermodynamic properties.

Measurement or Calculation of Thermodynamic Functions for Monolayer Formation

Purely thermodynamic measurements (not microscopic) have been used to determine parameters relevant to Figure 1. The literature is full of measurements of enthalpy and entropy

for common processes such as sublimation and boiling, and one can find heats of desorption (into vacuum) for a number of organic species. Heats of solution and desorption into organic solvents are less common, but some do exist. Examples of these are the work of Gamboa et.al [17] and of Matzger. [18] Gamboa reported heats of solution ($-\Delta H_{sol\text{-}crystal}$ in Figure 1) and solvation ($\Delta H_{vacuum\text{-}sol}$) for several transition metal tetraphenylporphyrins in chloroform. Heats of solution ranged from 55.6 kJ/mole to 14.5 kJ/mole, depending on the central metal. Barnard and Matzger used flow microcalorimetery to measure heats of adsorption ($\Delta H_{sol\text{-}mono}$) of 1-octadecanol, 1-octadecanethiol, stearic acid, octadecane, and 1-bromooctadecane from chloroform onto graphite. Their results ranged from -29.7 kJ/mole (for 1-bromooctane) to -70.3 kJ/mole (for 1-octadecanol).

Lackinger's group has contributed significantly to filling out the diagram in Figure 1 in the case of materials of interest in self-assembly studies. They identify their process as a "Born-Haber Cycle for Monolayers." [19-23] In general, they use temperature programmed desorption data to determine the heat of sublimation for a monolayer ($-\Delta H_{vac\text{-}mono}$), and the effusion rate from a Knudsen cell as a function of temperature to determine the enthalpy of sublimation ($\Delta H_{crys\text{-}vac}$). The temperature dependence of the absorbance of a saturated solution in the UV-visible region was used to determine the heat of solution ($-\Delta H_{sol\text{-}crystal}$). The estimation of the "dewetting" term is the most difficult. Lackinger defines dewetting as the process of removing the solvent from the substrate (a true dewetting) and then wetting adlayer of interest with solvent. Thus, the heats of wetting for the solvent on the substrate are overestimates of the net result of the multistep step "dewetting". Lackinger argues that for systems where the solvent does not order on the adlayer, one can estimate the dewetting term as the difference between the desorption enthalpy and the evaporation enthalpy.[22] If the solvent is weakly bound to both the bare substrate and the adlayer, this enthalpy will be very small. On the other hand, if the solvent forms a well defined structured monolayer on the substrate and weakly interacts with the solute adlayer, the dewetting term may be large, of the order of 10 kJ/mole. It should be noted that Lackinger often uses molecular dynamic and Monte Carlo calculations to estimate some of the more difficult thermal quantities, such as the solvent desorption energy. He says, "*The Achilles' heel of this approach is the semi-theoretical evaluation of the dewetting enthalpy which at this point necessarily relies on plausible assumptions*". [22]

The use of statistical mechanics to estimate adsorption entropies is another interesting feature of Lackinger's work. He uses the approach originally proposed by Whitesides and

coworkers. [24] This approach uses standard formulas for entropy of translation and of rotation, but takes into account the volume not occupied by solvent that is available to the solute. At equilibrium, when the concentration is just enough for a monolayer to form, $\Delta G_{sol\text{-}mono}$ should be zero and $T\Delta S_{sol\text{-}mono}=\Delta H_{sol\text{-}mono}$. If dewetting can be ignored, then $\Delta S_{sol\text{-}mono}$can be computed by considering the solute alone. If the dewetting term is important, the entropy change for dewetting must be included.[23] Thus, comparison of the calculated $\Delta S_{sol\text{-}mono}$ to the measured value of $\Delta H_{sol\text{-}mono}/T$ is an indicator of the role of the solvent in the overall process of monolayer formation. We note here that a series of determinations of $\Delta H_{sol\text{-}mono}$ and $\Delta S_{sol\text{-}mono}$ as a function of solvent would be an interesting study. Complicating such a study is the known occurrence of solvent dependent metastable polymorphs.[1,2,20,25] In some cases, these polymorphs can be traced to differing amounts of coadsorption of solvent.[25-27] In these cases, both enthalpy and entropy terms will strongly depend on the detailed nature of the solvent interaction. Figure 2 (taken with permission from reference 20) demonstrates a reversible phase transition for 1,3,5-tris(4-carboxyphenyl)benzene (BTB) in nonanoic acid. The authors conclude that solvent adsorption within the cavities of the low temperature "chicken wire" phase contribute sufficient enthalpy to outweigh the entropic cost at low temperature. At higher temperature the $T\Delta S$ outweighs the solvent heat of adsorption and the solvent molecules are replaced by BTB leading to the denser row structure seen at 55ºC.

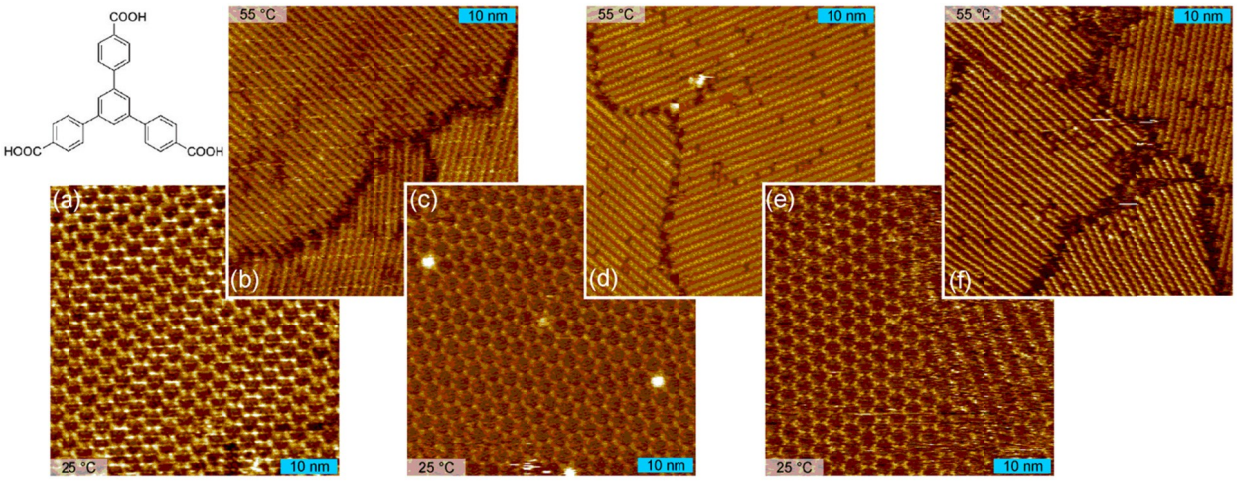

Figure 2. A temperature reversible phase transition in nonanoic acid. Image taken with permission from reference 20. Copyright 2010 American Chemical Society.

Solute Concentration and Phase Formation at Equilibrium

Before beginning this section, we should note that the use of equilibrium thermodynamic methods require that the system be in a state of dynamic equilibrium. There are many time stable systems that appear to be in equilibrium but that are not. For the studies reported in this section, dynamic equilibrium was either demonstrated or assumed.

The study of equilibrated surface structures as a function of concentration is a rich area for the application of thermodynamic principles. When two phases are in equilibrium on the surface and the adsorbate is also in equilibrium with the solution, equalities in chemical potential can be applied and extremely useful relations can be derived. An early example of such a study was the work of Matzger's group on competitive adsorption of alkyl dicarbamates on HOPG from phenyloctane solution.[28] They modeled the adsorption of each component with a Langmuir isotherm and used that model to determine the difference between the standard free energies of adsorption for pairs of adsorbates. They took X_i to be the mole fraction of the adsorbent i in solution, and θ_i to be the fraction of the surface covered by that component when in equilibrium with a solution having concentration X_i. By adjusting the solution concentrations ($X_i(\theta=0.5)$) such that there was equal coverage of each adsorbate, they were able to write:

$$\Delta\Delta G^0 \equiv \Delta G_2^0 - \Delta G_1^0 = RT \ln\left(\frac{X_2(\theta = 0.5)}{X_1(\theta = 0.5)}\right) \qquad (1)$$

Values of $\Delta\Delta G$ ranged from a high of 1.7 kJ/mole to near zero. Using the size of $\Delta\Delta G$ for various pairs of alkyl dicarbamates, one can determine the relative strength of adsorption for those pairs. Unlike the case of a mixture of n-alkanes, the alkyl dicarbamates studied by Matzger did not show a strong preference for longer molecules adsorbing more strongly than shorter ones.[28] Matzger attributes this to the hydrogen bonding between dicarbamates and the increased number of such bonds per unit area for the shorter chains.

Miyake and co-workers studied the coadsorption of various tetraphenyl porphyrins with long alkyl side chains on HOPG in phenyloctane solution.[29,30] Some of these were double decker complexes. Utilizing the contrast in STM images between the free base and the other compounds studied, they measured the ratio of metallated porphyrins and free base porphyrin both on the HOPG surface (θ_{free}, θ_{other}) and the concentration of these species in solution at room temperature. They found a non-linear relationship between the solution and surface concentrations. They assumed equilibrium between the surface and solution and used the

concentration variation to derive the difference in free energies of adsorption of the metallated and free porphyrins. They also identified the resulting value as ΔΔG.[29,30] In 2008, they performed a similar experiment with a Zn porphyrins complex and free base, and also found a non linear relationship between fraction in solution and fraction on the surface of HOPG. [31] In this paper, however, they realized that the assumption of equilibrium was not justified by their experiments and they refrained from associating the preferential adsorption with a ΔΔG value.

Another early example of the use of chemical potentials comes from the work of Lackinger's group.[32] They studied the complex coadsorption of benzenetribenzoic acid and trimesic acid at the liquid-HOPG interface in two different solvents (heptanoic and nonanoic acid). By varying the relative concentrations of the two acids in solution, they were able to observe six distinct phases. They used a simple model for the chemical potential of each component to help rationalize the complex phase diagram for this system.

A study of greater impact on understanding thermodynamics at the solution solid interface is the case of alkoxylated dehydrobenzo[12]annulenes (DBA-OCn) in trichlorobenzene (TCB) adsorbed on highly oriented pyrolytic graphite (HOPG).[33] At 21ºC in TCB, DBA adsorbs on HOPG in two different polymorphs depending upon the solution concentration. These structures are identified as a honeycomb phase with surface coverage Y_h, and a linear phase with coverage Y_l. Lei and coworkers [33] assumed that DBA behaved ideally on the surface such that the chemical potential of each phase would be given by $\mu_i = \mu_i^0 + RT\ln(Y_i)$. Similarly, the chemical potential of DBA in solution was written as $\mu_s = \mu_s^0 + RT\ln([DBA])$, where [DBA] is the molar concentration of DBA in solution. They then took into account the differing surface densities of the two phases by making the condition for equilibrium:

$$l\mu_l = h\mu_h + (l-h)\mu_s \qquad (2)$$

The coefficients l and h are needed to take into account the differing number of molecules per unit area for the two phases. Defining l and h as the number of molecules/nm^2 in the linear and honeycomb phases, respectively, the transfer of molecules to/from solution required by the phase change is recognized. Using eqn 2, the preceding assumptions, only considering complete surface coverage (so $Y_h+Y_l=1$), and defining m=l/h, they were able to derive an expression for the relative surface coverage as a function of solution concentration:

$$\ln\left[\frac{Y_h}{[DBA]}\right] = m\ln\left[\frac{1-Y_h}{[DBA]}\right] + \ln K \qquad (3)$$

Figure 3, taken with permission from reference 33, shows the experimental results plotted in the form suggested by eqn 3. Not only does the predicted coverage dependence follow equation 3, but the values of m extracted from the fit also agree well with the areas per molecule derived from the STM images. This demonstration that basic thermodynamics could be used to rationalize the equilibrium between phases was a major accomplishment.

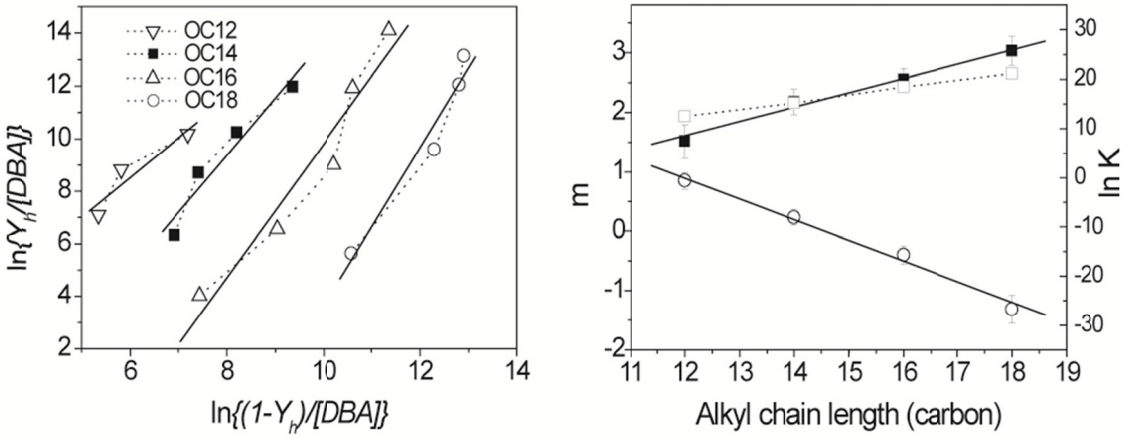

Figure 3. Fit of equation 3 to experimental data, taken with permission from reference 33.

The assumption that the chemical potentials of individual molecules on the surface must equal those in solution results in smooth variations of surface coverage with temperature. This did not occur in Bellec and coworkers' [34] study of molecules of 1,3,5-tristyrylbenzene substituted by alkoxy peripheral chains presenting n = 6, 8, 10, 12, or 14 carbon atoms (TSB3,5-Cn) adsorbed on HOPG from phenyloctane. They found that they could establish thermodynamic equilibrium between the solvent and two distinct low and high density phases and that the dominant phase depended strongly on solution concentration. In fact, they found a very sharp transition from the low density to high density phases with increasing concentration. This sharp transition could not be accounted for by Lei's model. Reasoning that islands of a given phase would be better treated as individual thermodynamic entities similar to how micelles are treated, [35,36] Bellec and coworkers modified the expression for the chemical potential to reflect this aggregate equilibrium:[34]

$$\mu_{i,N} = \mu^0_{i,N} + \frac{RT}{N}\ln(Y_i) \qquad (4)$$

Where N is the number of molecules in a particular island of phase i. With this one change, they were able to derive an equilibrium expression for islands containing N molecules in equilibrium with solution:

$$K = \frac{Y_l^{1/N} c^{k-1}}{Y_h^{k/N}} \qquad (5)$$

Where k is defined as the area per molecule of the low density (porous) phase divided by the area per molecule of the high density phase. Bellec and coworkers then assume that so long as N is sufficiently large for most islands, the behavior of the assembly of islands will be reflected in equation 5 with a single value of N.[34] Figure 4 shows the evolution of the predicted coverage of the porous structure (Y_l) with solution concentration and N. The triangular symbols represent the experimental data. Once N is greater than about 20, a well defined phase transition develops in the theoretical expression and accurately reflects the experimental data. Thus, it is possible to accurately model discrete changes in surface structure with concentration.

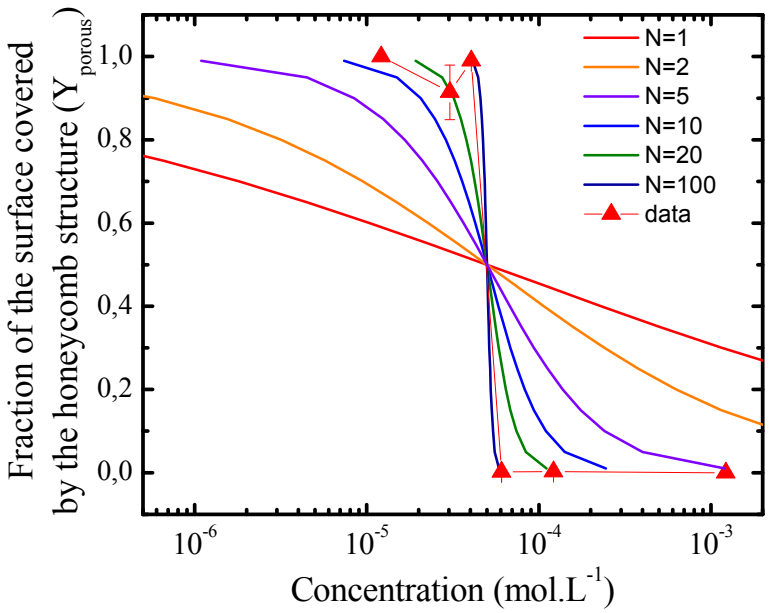

Figure 4. Fit of experimental data for adsorption of TSB to equation 5. Taken with permission from reference 34. Copyright 2011 AIP Publishing LLC.

Temperature and Concentration at Equilibrium

The next level in treating equilibrium surface processes by thermodynamics is to compare both concentration and temperature dependences in the data and as predicted by a thermodynamic model. De Feyter's group took up this challenge by studying the DBA phase transformation as a function of temperature.[37] In addition, they took into account the fact that 19 molecules of solvent (TCB) per two DBA were adsorbed in the pores of the low density structure. Defining C_0 as the concentration (at a given T) where Y_l=Y_h, (equal surface coverage of the phases), and using Bellec's treatment of the chemical potentials, they found

$$\ln C_0 = \frac{1}{RT}\left(-\Delta H_h^0 + \frac{\left(\Delta H_l^0 - \Delta H_h^0\right)}{m-1}\right) + \frac{\Delta S_h^0}{R} - \frac{\left(\Delta S_l^0 - \Delta S_h^0\right)}{(m-1)R} - \frac{19\Delta S_{TCB}^0}{2(m-1)R} \qquad (6)$$

where the ΔH_i^0 terms are the standard enthalpies for desorption of the indicated low or high density phase, the ΔS_i^0 are the entropies of desorption for the respective phases, and ΔS^0_{TCB} is the entropy for desorption of a mole of solvent. Equation six predicts that a plot of $\ln(C_0)$ versus 1/T should yield a straight line. Figure 5 (reproduced with permission from reference 37) presents the experimental data and a best fit straight line. The slope is found to be -155. kJ/mole and the intercept is 384 J/mole-K. Attempts to reproduce these values through the use of molecular mechanics for the enthalpy and a Lackinger style calculation of the entropy were not successful.

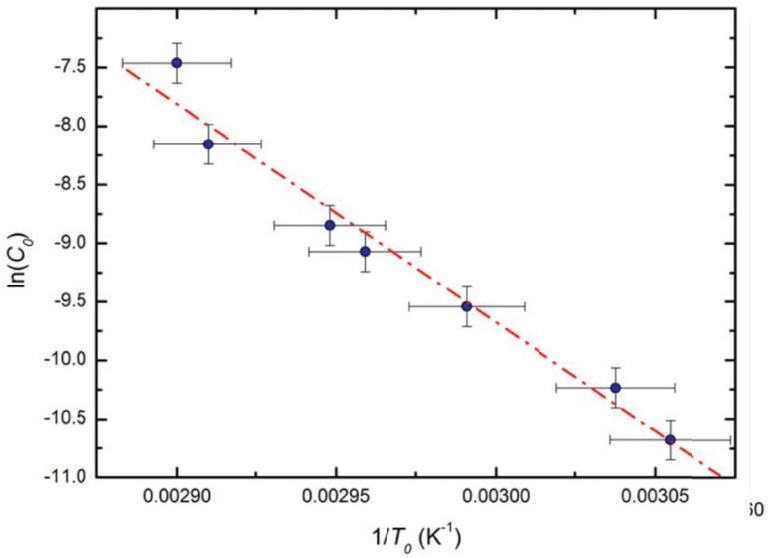

Figure 5. Fit of equation 6 to experimental data for DBA on HOPG. Taken with permission from reference 37. Copyright 2013American Chemical Society.

De Feyter explained the discrepancy between experimental and modeling results as due to residual motion of TCB molecules in the DBA pores of the low density phase. They also believe that the rotational entropy of both DBA and TCB were overestimated by the method used. Further, they caution that there can be large errors in the conformational entropy.

A very different equilibrium system that has been analyzed both in terms of concentration (pressure in this case) and temperature is the oxygen binding of cobalt octaethylporphyrin (CoOEP) monolayers.[5] In solution at room temperature, CoOEP cannot bind O_2. A monolayer of CoOEP on Au(111) does not bind O_2 down to -25°. [38] A monolayer of CoOEP on HOPG, however, does bind O_2. Friesen and co-workers have not only imaged the binding, but have also established that it is in fact a dynamic equilibrium process. Figure 6 shows two sequential STM images acquired a few minutes apart from a sample consisting of CoOEP supported on HOPG and covered by phenyl octane in an atmosphere of 176 Torr O_2 and held at 25ºC. The very bright object in each image is an impurity used as a spatial reference. O_2 binding by CoOEP reduces the resonant tunneling through the Co(II) ion and makes the bound molecules appear dark. Each O_2-CoOEP in a given scan is identified by its "loss of height" and is circled in Figure 6. The ones with white circles are the same molecules in both scans. Those marked with purple circles are different molecules in the later scan than in the first. As time evolves further images were taken and the dynamic variation of O_2 binding sites was observed.

Defining θ as the ratio of O_2-CoOEP to the total number of molecules in a given image, one can plot the variation of observed coverage with time as is done in the bottom half of Figure 6. As is required by the small sampling size (a few hundred molecules in each image), the value of θ fluctuates, but the average value is quite stable. Thus, there is a dynamic exchange of O_2 between the gas (and solution) phases and the bound state. This is a clear proof of a dynamic equilibrium process. Extending arguments derived from solution phase studies such as those of Collman [39,40] and Stynes,[41] it appears that the HOPG surface is donating electrons to the cobalt center thereby stabilizing the polarized Co-O_2 complex.

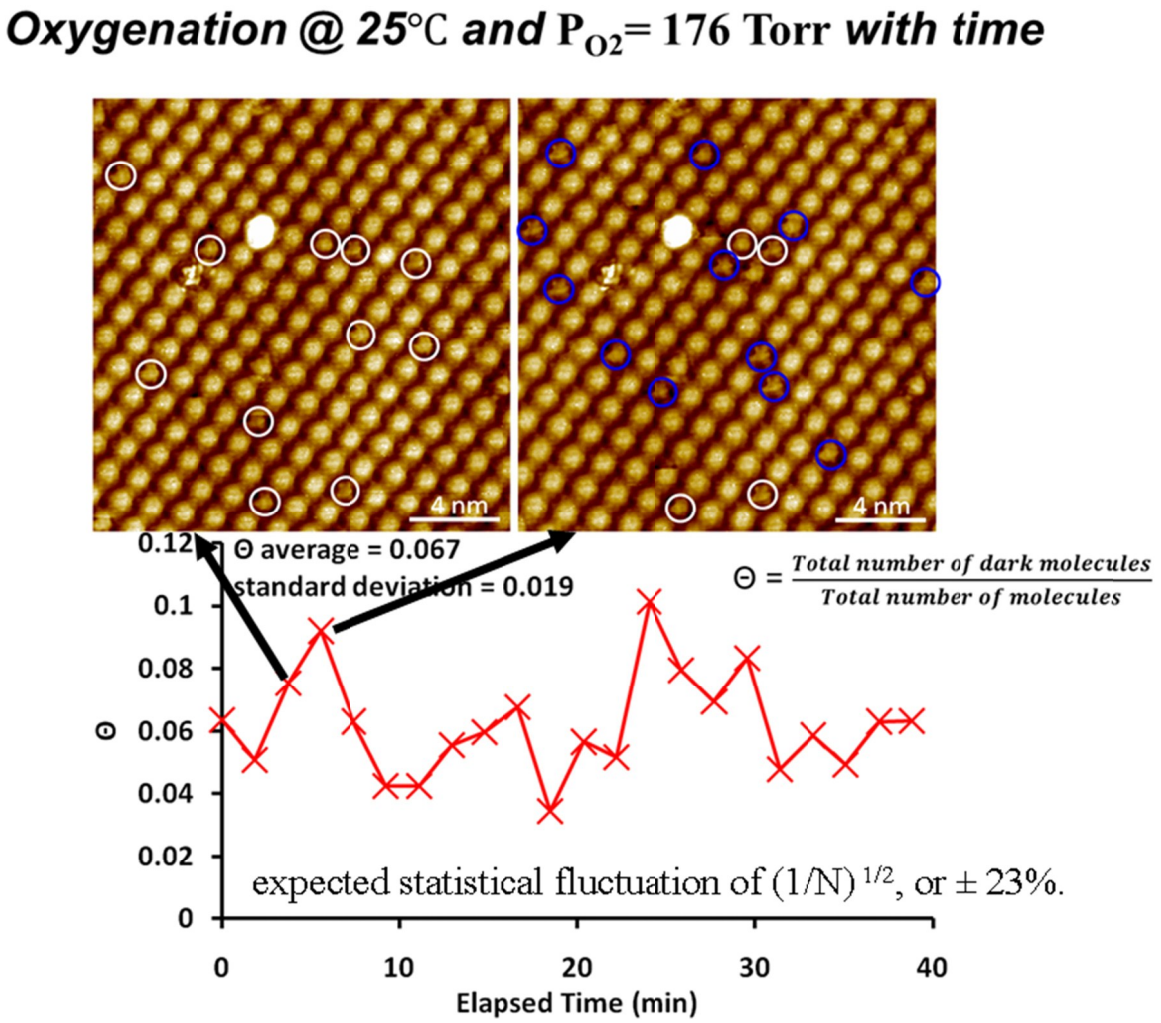

Figure 6. Sequential images of the CoOEP/HOPG surface in phenyloctane and in equilibrium with oxygen. Each point in the surface coverage versus time graph is derived from an STM image. Circled molecules are those which are bound to oxygen. Note that these change with time but that the average is stationary – this demonstrates dynamic equilibration. N is the number of molecules in each image. Reprinted with permission from reference 5. Copyright 2012 American Chemical Society.

If one increases the partial pressure of O_2 at fixed temperature, the value of θ increases and follows a Langmuir isotherm. That is:

$$K(T) = \frac{\theta(T)}{\left(1-\theta(T)\right)\left(P/P^0\right)} \qquad (7)$$

where K(T) is the equilibrium constant for the process:

$$O_{2(g)} + \text{CoOEP/HOPG} = O_2\text{-CoOEP/HOPG} \qquad (8)$$

and $\Delta G^0 = -RT\ln(K(T))$ for the process described in equation 8. It is conventional to take $P^0 = 1$ Torr.

By repeating this sequence of time elapse experiments at various temperatures and pressures, a graph of ΔG^0 versus T can be generated as in Figure 7.[5] One observes an essentially linear variation in ΔG^0 as a function of temperature. Since $\Delta G^0 = \Delta H^0 - T\Delta S^0$, the slope of the curve is equated to ΔS^0 and ΔH^0 can then be determined. The value of ΔH^0 (-68 kJ/mole) is more negative than the larger values reported for cobalt complexes in solution (about -60 kJ/mol), but is consistent with the unusually large binding and long residence time observed for O_2 on CoOEP/HOPG. The value of ΔS^0 [-297 J/(mol K)] is more negative than previous reports for solution phase state binding by cobalt complexes [about -230 J/(mol K)], and also slightly larger than the negative of the absolute entropy for the O_2 molecule at 1 Torr and 298 K calculated from statistical mechanics (-268 J/mol K). However, when one considers the error bars in Figure 7, values of $\Delta S^0 = -268$ J/mol K and $\Delta H^0 = -60$ kJ/mole are acceptable.

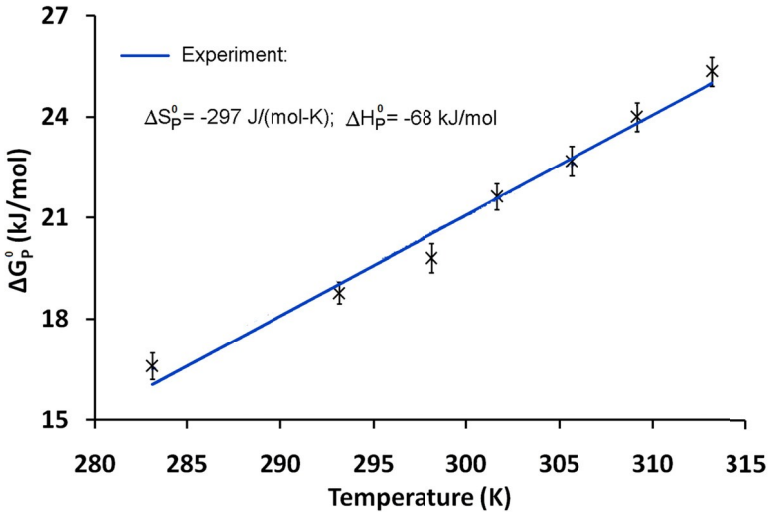

Figure 7. Graph of ΔG_P^0 derived from Langmuir equilibrium constants at various temperatures. Fit of $\Delta G = \Delta H - T\Delta S$ is shown. Taken with permission from reference 5. Copyright 2012 American Chemical Society.

To our knowledge, this was the first example of extracting all the principal thermodynamic functions for a chemical process at the solution-solid interface by STM. These results both demonstrate the potential power of the technique and point out a weakness. Because the values of ΔS^0 and ΔH^0 depend on the temperature dependence of ΔG^0, accurate values will require measurements over large temperature regions or the measurement of hundreds of thousands of surface sites at precisely known temperatures in order to reduce the uncertainties in the values of ΔG^0.

It is important to note that molecular time dependent images allow one to guarantee a state of dynamic equilibrium, rather than having to assume it. As we shall see in later sections, time dependent imaging can be used very effectively in identifying kinetically controlled processes.

Time elapsed imaging also was used to study the reaction processes between O_2 and a manganese porphyrin (MnP) supported on HOPG in a solution-surface experiment utilizing octanoic acid as solvent. [42] While they did not extract thermodynamic data from the images, they did use them to help elucidate the complex chemistry that occurs on the manganese ion site.

Recognition of Competition Between Kinetics and Thermodynamics

While quantitative measurement of kinetic parameters associated with processes at the solution-solid interface are just becoming available, it has been recognized by several authors that a competition between kinetic and thermodynamic driving forces was occurring. An early example of this realization was the study of Piot et al.[43] They present a systematic investigation of the structural evolution of hexakis(n-dodecyl)-peri-hexabenzocoronene (HBC-C12) on an n-$C_{50}H_{102}$ monolayer on HOPG from n-tetradecane as solvent, with the alkane acting as a template. The growth of the HBC monolayer is slow enough that it can be followed over several hours. A time dependent progression through an initial phase, into an intermediate phase, and then finally a third stable phase was observed. They interpreted these observations as due to phases separated by kinetic barriers where the activation energies were comparable to kT. The initial phase is the least densely packed and the final phase has the highest density. Because the initial (kinetically controlled) phase is the only phase seen on HOPG, they suggest that room T adsorption of HBC-C12 is entirely kinetically controlled on HOPG and that the barrier to conversion is >> kT. In the Bellec study mentioned earlier, TSB3,5-C*n* in phenyoctane on HOPG was studied on HOPG in the temperature range from 273 K to 338 K.[34] By controlling the thermal history, they were able to create non-equilibrium distributions of the high and low density phases. They state that the coexistence of domains of individual phases results from a kinetic blockade rather than equilibrium. They further observe that the number of initially formed grains reflects nucleation rate and the size of the domains reflects growth rate. The size and phase of these grains is extremely important because the strongly H-bonded networks undergo phase change much more quickly at the domain boundaries rather than internally.

In a study of a mixed monolayer of cobalt tetraphenylporphyrin (CoTPP) and ZnTPP from low concentration benzene solutions onto Au(111), phase separation of the two complexes was observed. [44] In understanding this study, it is important to note that the Au(111) surface shows a 22x$\sqrt{3}$ reconstruction with a long range herring bone patters created by both FCC and HCP regions.[45] Thus, the observed phase separation was attributed to CoTPP binding preferentially to

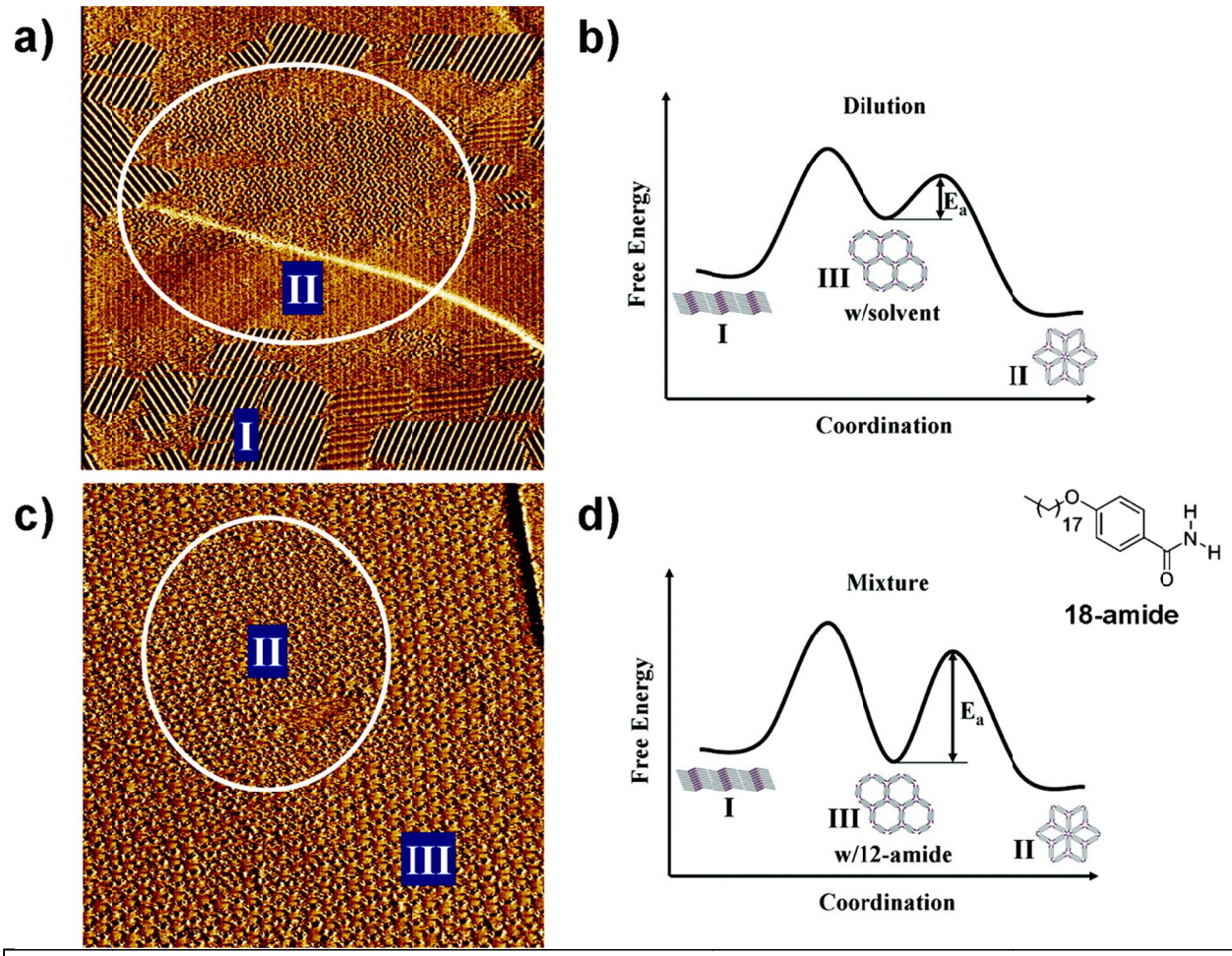

Figure 8. STM images ((a) 400 × 400 nm2, (c) 200 × 200 nm2) and reaction coordinate diagram of the phase transformation from (a, b) the homogeneous solution of 25 μM and (c, d) the mixture of 1:3 (18-amide/12-amide) with 25 μM of 18-amide. Solvent used was phenyloctane. Reproduced with permission from reference 47. Copyright 2012 American Chemical Society.

FCC sites while ZnTPP binds more strongly but non-preferentially. At higher concentrations, the adlayer was ordered but compositionally disordered. They use this concentration dependent change in surface structure to postulate that the low concentration film is kinetically controlled while the high concentration adlayer is thermodynamically controlled. Considering later quantitative experiments by Bhattarai and coworkers to be discussed later in this section, [6] it is more likely that neither structure is an equilibrium structure.

A particularly extreme case of kinetic barriers affecting polymorphism was presented by Ahn et al in the form of a C_s-symmetric amide amphiphile containing a C_{18} alkyl chain (see Figure 8) that exists in at least six crystalline phases at the liquid/solid interface at room temperature.[46] These phases depend upon concentration and time. Some of the phases demonstrated concentration dependent stabilities while others were purely kinetic in origin. These transformations are interpreted in terms of a complex activation energy pathway involving

more than one local minimum. The same group later demonstrated that additives could be used to dramatically affect the phase transformation rates (see Figure 8).[47] For example, the transformation rate from phase III to phase II was found to decrease 10 fold with the addition of 12-amide to the 18-amide in phenyloctane solution.

While the study of Haxton and coworkers is a UHV rather than solution phase effort, it does demonstrate that the competition between kinetic and thermodynamic processes can play a significant role on adsorption. Using a combination of STM and theoretical (*ab initio* and statistical mechanical modeling) methods, Haxton and coworkers studied the adsorption of 1,4-benzenediamine (BDA) on Au(111) in UHV.[48] Of the many possible hydrogen bonded BDA nanostructures, the interplay of intermolecular forces, assembly dynamics, and surface modulation select for thermodynamically stable linear chains and kinetically preferred branched chains.

Strong Kinetic Control

A particularly interesting observation concerning the stabilization of a metastable polymorph comes from the De Feyter group. [49] They used directional solvent flow to force a metastable phase (not normally stable at the temperature studied) into supersized domains formed on a nearly dry sample. The metastable polymorph could be rapidly converted to the stable form by the simple act of addition of a drop of solvent to the surface. Clearly this allowed the adsorption/desorption processes to reestablish equilibrium. The very large size of the metastable domains likely plays a role as well. Since structural changes often occur most rapidly at domain boundaries, the absence of such boundaries and defects is expected to result in a very high barrier for phase transformation in the dry film. An interesting counterpoint to this issue of phase transformation in dried films is the conversion of CuPcOC8 (Figure 9) films on HOPG initially deposited from toluene solution but dried and heated before imaging.[50] The thermodynamically stable state (the hexagonal structure) is not the only phase formed at room temperature. Rather, one observes a mixture of grains of a kinetically favored quartic phase with grains of the hexagonal phase. At room temperature the quartic phase is favored (3:1). With time and with heating, however, the dry film will convert to the thermodynamically favored hexagonal phase. Because the film is dry, it must result from in situ reconstruction rather than the more normal process of Ostwald ripening[51-53] (Desorption from small grains favored over

adsorption on the boundaries of large grains). This type of dry reconstruction is likely due to the small grain size of the cast film.

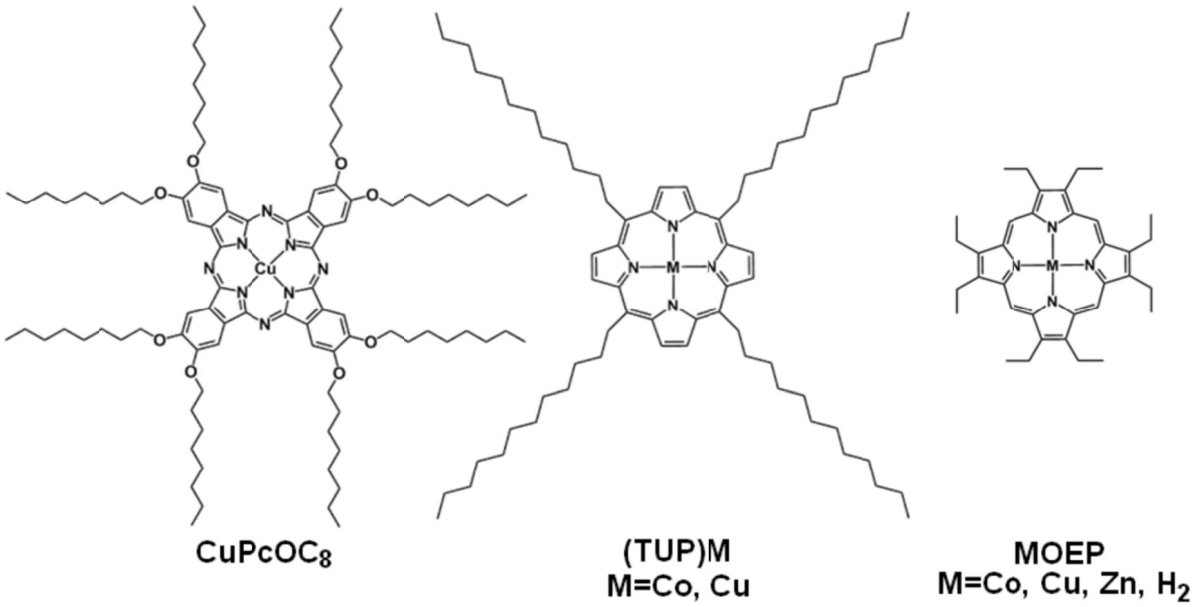

Figure 9: Models of selected compounds.

Another example of the relative kinetic control of adsorbates on surfaces comes from the work of Coenen and coworkers.[54] They observed the behavior of monolayers of copper 5,10,15,20-tetraundecylporphyrin ((TUP)Cu, Figure 9) at the octanoic acid-HOPG interface. As expected, these tetralkyl substituted porphyrins quickly form large domains of well ordered molecules with heavily interdigitated alkyl chains. Within seconds, they assemble into one of two concentration dependent surface polymorphs. These structures are easy to differentiate since one polymorph is about 0.4 molecules/nm^2 while the other is close to 0.3 molecules/nm^2. As expected, the high density structure is the one observed at higher solution concentration. Based on the work of Bellec,[34] DeFeyter,[37] and others reported above,[28-34] one might attribute this to yet another concentration dependent equilibrium between two polymorphs. Such is not the case. If one prepares the low density phase and then covers it with high concentration solution, regions of the low density phase persist even after 16 hours. This suggests strongly that the surface molecular structures are not in equilibrium with the solution, but rather are determined by the kinetics of the adsorption process. By exposing the (TUP)Cu low density surface to a solution of (TUP)Co, the authors were able to both prove their assertion and identify the mechanism of the

very slow equilibration process. Cobalt porphyrins and phthalocyanines are well know to appear to have very bright centers in STM images at moderate voltages, while copper and nickel porphyrins and phthalocyanines appear dark.[6,55-58] If there is exchange between the surface and solution, the bright cobalt porphyrins should replace the dim copper complexes at the rate of the exchange. Moreover, since the (TUP)Co concentration was high, at least some of the bright structures should be the high density phase. What is observed is a very slow build up of (TUP)Co and the high density phase only in the vicinity of certain defects in the low density phase. Insertion into regions that are defect free only occurs in 2-3% of the total cobalt insertion sites.

Ferreira and coworkers report an interesting case of delayed then rapid conversion between a kinetically controlled and a thermodynamically stable phase. [59] The adsorption of ZnOEP onto HOPG from n-tetradecane first yields a metastable α-phase. Then, about 2 hours later there is a rapid conversion to the stable β-phase. They fit the relative coverage of β-phase (θ_β) as a function of time with the expression:

$$\theta_\beta = \theta_0 + \theta_{\max}\left(1 - e^{k(t-t_c)}\right) \qquad (9)$$

Where $\theta_0=10^{-5}$, θ_{max} = 1, t_c = 121 min, and k = 0.0023/s. They attribute the long delay, t_c, to a nucleation time for the β-phase in the α-phase.

The most extreme version of kinetic control is when there is no desorption at all. In these cases, only the initial structure formed during adsorption, nucleation, and grain growth is observed. If adsorption follows first order kinetics, for a single solute species:

$$\frac{d\theta}{dt} = k^a M(1-\theta) \qquad (10)$$

where M is the molarity of the solute, k^a is the adsorption rate constant, and θ is the fractional surface coverage. For two components, C and N, where adsorption is fast and desorption is slow to extremely slow:

$$\frac{d\theta_N}{dt} = k_N^a X_N M(1-\theta) \qquad (11)$$

$$\frac{d\theta_C}{dt} = k_C^a X_C M(1-\theta) \qquad (12)$$

Where M is the total solute molarity, X_i is the number of moles of i divided by the total number of moles of solute in solution, and θ_i is the fraction of surface covered by species i. Combining these, yields the equation for the overall surface coverage:

$$\theta = (1 - e^{-\bar{k}Mt}) \qquad (13)$$

where $\bar{k} = \left(k_N^a X_N + k_C^a X_C\right) = k_N^a X_N + k_C^a (1 - X_N)$. Substituting this back into the rate equations for the individual components, we find that at steady state:

$$\theta_N = \left(\frac{k_N^a X_N}{\bar{k}}\right) = K_N X_N \qquad (14)$$

$$\theta_C = \left(\frac{k_C^a X_N}{\bar{k}}\right) = K_C X_C \qquad (15)$$

Or that

$$\frac{\theta_N}{\theta_C} = \frac{k_N^0 X_N}{k_C^0 X_C} \qquad (16)$$

which has exactly the same form as that for a two component system at thermodynamic equilibrium (eq 1). Thus, simply comparing steady state surface coverage and solution concentration cannot be used to determine if a particular structure is kinetically or thermodynamically driven.

An excellent example of this is given by the 2 component system of cobalt octaethylporphyrin (CoOEP) and NiOEP (Figure 9) in phenyloctane at the solution-Au(111) interface.[6] Figure 10 shows STM images taken at three different relative solution concentrations. As mentioned above, the CoOEP are easily distinguished from the NiOEP by their high apparent height. The ratio of bright to dark molecules in each image equals the ratio of CoOEP and NiOEP in the covering solution. Thus, either $\Delta\Delta G = 0$ (from eqn 1), or the rates of adsorption are the same for each species, or maybe the system is evolving between those two limits.

In order to determine the actual nature of the surface formation process, time evolution studies are essential. If the system is at equilibrium, molecules on the surface should blink as CoOEP is exchanged for NiOEP. When such a movie is made, even up to temperatures of 343 K, there is no evidence of any blinking, on a time scale of 10 minutes or so.[6] Thus the activation energy barrier is much greater than 343k. It is not until about 383 K that one begins to see some small amount of exchange, and it requires heating to above 400 K before significant exchange occurs on the scale of hours. In order to quantitatively determine the desorption rate, the following experiment was performed. A monolayer of CoOEP was prepared at room temperature and then covered with a solution containing a large excess of NiOEP. This solution was heated to 408K for different fixed periods of time, cooled to room temperature, and then θ_N was determined (see Figure 11). Because the desorption rate is negligible below 373 K, and very slow even at 408 K, the value of θ_N determined in this way should be very close to the value determined at 408 K at time t. With these assumptions and the fact that the adsorption rates are orders of magnitude greater than the desorption rates, one can derive an expression for the fraction on the gold surface initially covered by CoOEP that is replaced by NiOEP after time t. [6]

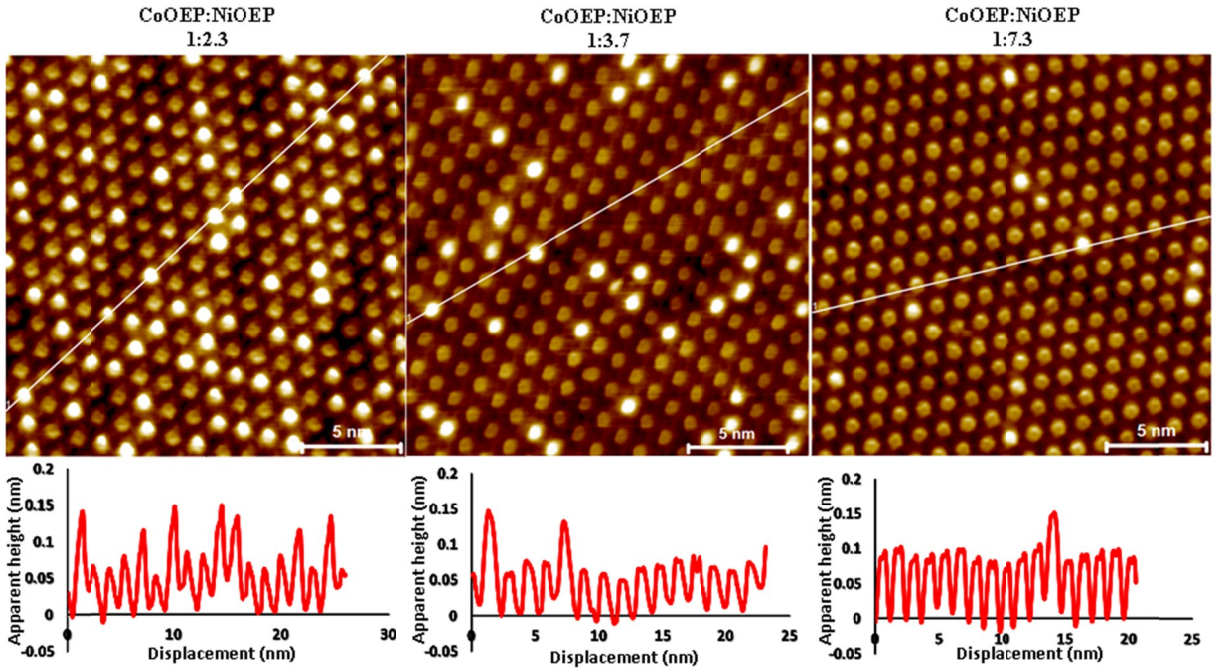

Figure 10. Effect of relative CoOEP to NiOEP solution concentration on the constant current STM images obtained. Reprinted with permission from reference 6. Copyright 2014 American Chemical Society.

This expression is:

$$\Theta_N = (\frac{1}{b})(1 - e^{-bk_C X_N t}) \quad (17)$$

Where

$$b = \left[(\frac{k_N^d}{k_C^d X_N})(1 - X_N) \right] + 1 \quad (18)$$

Figure 12 is a plot of the observed values of θ_N as a function of time at 408 K. The blue, red, and black curves are theoretical curves generated from eqn 17 for differing values of k_N^d/k_C^d, and of k_C^d. It turns out that the fit for the desorption rate of CoOEP (k_C^d) is very well defined, but that k_N^d is poorly defined. Reversal of the experiment by starting with a NiOEP monolayer exposed to a solution rich in CoOEP would allow precise determination of k_N^d, but interpretation is much more complicated in this case of site specific desorption rates.. The rate of desorption of CoOEP from a Au(111) surface in contact with phenyloctane solution at 408 K is only 6.7×10^{-5}/s. If one takes the attempt frequency for the desorption to be of the order of 10^{12}/sec, one can estimate the barrier to desorption (the desorption activation energy) to be 1.3 eV or 125 kJ/mole. It is also interesting to note that the observed desorption rate is orders of magnitude slower than for a covalently bound thiol at 25°C (0.42/s for octanethiol).[60]

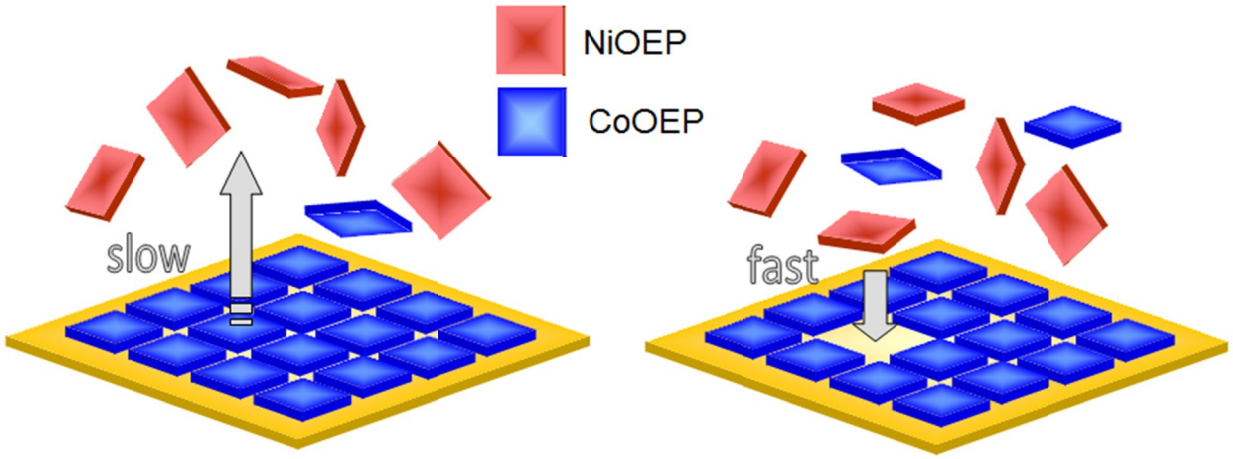

Figure 11: Tracking desorption from a solution-solid interface. Reprinted from reference 6. Copyright 2014 American Chemical Society.

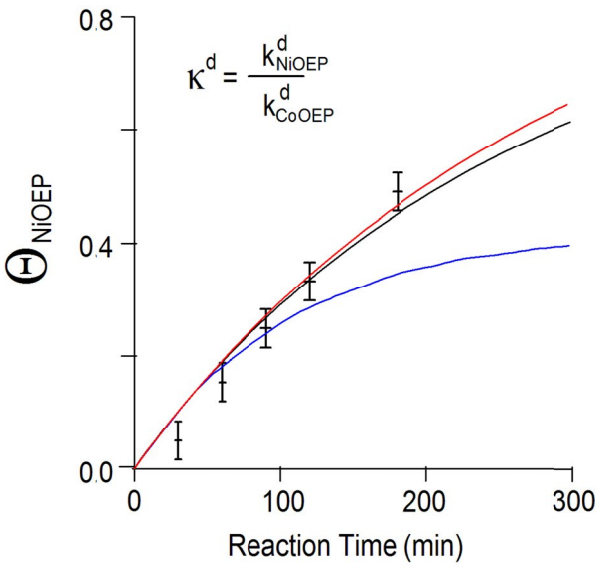

Figure 12: NiOEP coverage with reaction time at 135°C. k_C^d=0.004/min, Red : κ^d=0.1,; black: κ^d=1.0; blue: κ^d= 10. Reprinted with permission from reference 6. Copyright 2014 American Chemical Society.

One important potential pitfall in these time kinetic measurements is a change in monolayer composition generated by a tip induced surface change. Tip-induced effects have been used in the reversible isomerization of azobenzene[61], polymerization of organic molecules,[62] manipulation of the reconstruction of Au(111),[63] inducing chemical reaction at the organic-metal interface,[64,65] and many other applications. Most relevant to this work are reports of tip-induced surface desorption of porphyrins and porphyrin like materials. In porphyrins, it has been shown that this desorption process can occur via two different mechanisms; (i) either by applying a pulse of high voltage (>|2| V) to the tip,[66] (ii) or by scanning at a low bias voltage such that the tip-surface separation is very low in which case the adsorbed molecules are physically removed by the tip.[67] In either case the newly exposed substrate will be rapidly covered by adsorption from the solution in actual contact at that time. Our experience, and those of others, is that these effects are limited to about 50 nm in the case of a voltage pulse. [61,62,66] In the case of physical contact between the tip and adlayer, the disrupted area can be as large, or somewhat larger, as the scan area. The adverse effects of tip-surface interaction in the kinetic studies described here can be easily detected and images containing them eliminated from analysis. It is also critical to immediately move to a new location to continue data analysis.

Wide ranging opportunities!

34% of the papers cited in this review were printed in 2013 or 2014, and only 19% were published before 2000. These numbers only indicate the trend since the quantitative nature of the literature is also changing. The ability to extract real quantitative kinetic and thermodynamic data is just emerging, but the need for that data is critical. The rational design of ordered and stable structures at the solid solution interface absolutely requires the ability to quantitatively predict, or effectively estimate, the kinetic and thermodynamic parameters that control adlayer

formation. At the current time, too few of these important quantities are known – so few that no convincing test of theoretical models can be offered. The good news is that this condition is rapidly changing. Several groups around the world have turned their attention to the very physical chemistry of adlayer formation at the molecular level and are beginning to provide clear evidence of the relative importance of kinetic and thermodynamic factors. More than that, quantitative rate constants and functions of state are being measured for select systems and those efforts are accelerating. The roles played of solvent, substrate, temperature, and pressure are slowly being unraveled for selected model adsorbates. The next few years should see a dramatic increase in our fundamental knowledge about non-covalent adlayer formation at the solution-solid interface.

Acknowledgement

The US National Science foundation generously provided support for this work in the forms of grants CHE-1403989 and CHE-1112156. We also gratefully acknowledge the assistance of Mr. Ashish Bhattarai.

[1] K.S. Mali and S. De Feyter, *Phil Trans R Soc A*, 2014, **371**: 20120304.

[2] R. Gutzler, L. Cardenas and F. Rosei, *Chemical Sciences*, 2011, **2**, 2290-2300.

[3] J. M. MacLeod and F. Rosei, *Australian Journal of Chemistry* 2011, **64**, 1297-1298.

[4] K. S. Mali and S. De Feyter. *Phil Trans R Soc A***,** 2013, **371**, 20130263.

[5] B. A. Friesen, A. Bhattarai, K. W. Hipps, and U. Mazur, *J. Amer. Chem. Soc.***,** 2012, **134**, 14897-14904.

[6] A. Bhattarai, U. Mazur, K. W. Hipps, *J. Amer. Chem. Soc*., 2014 **136** (5), 2142–2148.

[7] Lindsay, Stuart M. (Molecular Imaging Corporation, USA). U.S. **(1997)**, 11 pp. CODEN: USXXAM US 5654546 A 19970805 Patent written in English. Application: US 95-551836 19951107.

[8] F. Oulevey, G. Gremaud, A. J. Kulik, B. Guisolan. *Review of Scientific Instruments,* 1999, **70**, 1889-1890.

[9] M. Trawick, D. E. Angelescu, P. M. Chaikin, M. J. Valenti, R. A. Register. *Review of Scientific Instruments,* 2003, **74**, 1390-1392.

[10] A. Jahanbekam, U. Mazur, and K. W. Hipps, *Rev. Sci. Instrum.,* 2014, **85**, 103701.

[11] W. Song, N.Martsinovich, W. M. Heckl, and M. Lackinger, *J. Amer. Chem. Soc*., 2013, **135**, 14854-14862.

[12] H. Marbach and H. P. Steinruck, *Chem. Commun.,* 2014, **50**, 9034-9048

[13] W. A. English and K.W. Hipps, *Journal of Physical Chemistry C*, 2008; **112**(6); 2026-2031.

[14] C. Marie, F. Silly, L. Tortech, K. Mullen, and D. Fichou, *ACS Nano*, 2010, **4**, 1288-1292.

[15] K. S. Mali, L. Zophel, O. Ivasenko, K. Miillen, and S. De Feyter, *Chem. Asian J*, 2013, **8**, 2497 -2505.

[16] F. Hu, Y. Gong, X. Zhang, J. Xue, B. Liu, T. Lu, K. Deng, W. Duan, Q. Zeng and C. Wang, *Nanoscale*, 2014, **6**, 4243–4249.

[17] M. Gamboa, M. Campos, and L. Alfonso Torres, *Inorg. Chem.,* 2010, **49**, 659–664.

[18] R. A. Barnard and A. J. Matzger, *Langmuir* 2014, **30**, 7388-94

[19] W. Song, N. Martsinovich, W. M. Heckl, and M. Lackinger, *J. Amer. Chem. Soc.***,** 2013, **135**, 14854-14862.

[20] R. Gutzler, T. Sirtl, J. F. Dienstmaier, K. Mahata, W. M. Heckl, M. Schmittel, and M. Lackinger, *J. Amer. Chem. Soc.*, 2010, **132**, 5084–5090.

[21] W. Songab, N. Martsinovichd, W. M. Hecklabc, and M. Lackinger, *ChemComm,* 2014, **50**, 13465,13468.

[22] W. Song, N. Martsinovich, W. M. Hecklabe and M. Lackinger, *Phys.Chem.Chem.Phys*., 2014, **16**, 13239.

[23] W. Song, N. Martsinovich, W. M. Heckl, and M. Lackinger, *ChemComm*, 2014, **50**, 13465-13468.

[24] M. Mammen, E. I. Shakhnovich, J. M. Deutch, and G. M. Whitesides, *J. Org. Chem*., 1998, **63**, 3821-3830.

[25] T. Sirtl, W. Song, G. Eder, S. Neogi, M. Schmittel, W. M. Heckl, and M. Lackinger, *ACS Nano,* 2013, **7**, 6711-6718.

[26] B. Gyarfas, B. Wiggins, M. Zosel, and K. W. Hipps, *Langmuir*, 2005, **21**, 919-923.

[27] A. Jahanbekam, S. Vorpahl, U. Mazur, and K W Hipps, *J. Phys. Chem. C*, 2013, **117***,* 2914-2919.

[28] K. Kim, K. E. Plass, and A. J. Matzger, *J. Am. Chem. Soc.,* 2005, **127**, 4879-4887.

[29] T. Ikeda, M. Asakawa, M. Goto, K. Miyake, T. Ishida, and T. Shimizu. *Langmuir,* 2004, **20**, 5454-5459.

[30] J. Otsuki, S. Kawaguchi, T. Yamakawa, M. Asakawa, and K. Miyake, K. *Langmuir,* 2006, ***22***, 5708-5715

[31] T. Ikeda, M. Asakawa, K. Miyake, M. Goto, and T. Shimizu. *Langmuir,* 2008, **24**, 12877-12882

[32] L. Kampschulte, T. L. Werblowsky, R. S. K. Kishore, M. Schmittel, W. M. Heckl, and M. Lackinger, *J. Am. Chem. Soc.*, 2008**, 130**, 8502–8507.

[33] S. Lei, K. Tahara, F. C. De Schryver, M. Van der Auweraer, Y. Tobe, and S. De Feyter, Angew. *Chem. Int. Ed*.**,** 2008, **47**, 2964 –2968.

[34] A. Bellec, C. Arrigoni, G. Schull, L. Douillard, C. Fiorini-Debuisschert, F. Mathevet, D. Kreher, A. Attias, and F. Charra, *J. Chem. Phys*. 2011, **134**, 124702.

[35] "The Hydrophobic effect: Formation of Micelles and Biological Membranes" by Charles Tanford, Second edition, John Wiley & Sons publication, 1973.

[36] J. Israelachvili, *Langmuir,* 1994, **10**, 3774-3781.

[37] M. O. Blunt, J. Adisoejoso, K. Tahara, K.Katayama, M. Van der Auweraer, Y. Tobe, and S. De Feyter, *J. Am. Chem. Soc.*, 2013, **135**, 12068-12075.

[38] A. Bhattarai and K. W. Hipps, private communication.

[39] J. P. Collman, J. I. Brauman, K. S. Suslick, *J. Amer. Chem. Soc.*, 1975**, 97***,* 7185-7186.

[40] J. P. Collman, J. I. Brauman, K. M. Doxsee, T. R. Halbert, S. E. Hayes, and K. S. Suslick, *J. Amer. Chem. Soc.,* 1978**, 100***,* 2761-2766.

[41] D. V. Stynes, H. C. Stynes, B. R. James, and J. A. Ibers, *J. Amer. Chem. Soc*.**,** 1973**, 95***,* 1796-1801.

[42] D. den Boer, M. Li, T. Habets, P. Iavicoli, A. E. Rowan, R. J. M. Nolte, S. Speller, D. B. Amabilino, S. De Feyter and J. A. A. W. Elemans, *Nature Chemistry***,** 2013, **5**, 621-627.

[43] L. Piot, A. Marchenko, J. S. Wu, K. Mullen and D. Fichou, *J. Am. Chem. Soc*., 2005, **127**, 16245.

[44] K. Suto, S. Yoshimoto, and K. Itaya, *Nanoscience and Nanotechnology***,** 2009, **9**, 288-294.

[45] F. Hanke and J. Bjork, *Phys. Rev. B*, 2013, **87**, 235422 (1-6).

[46] S. Ahn and A. J. Matzger, *J. Amer. Chem. Soc.*, 2010, **132**, 11364–11371.

[47] S. Ahn and A. J. Matzger, *J. Am. Chem. Soc*., 2012**, 134**, 3208−3214.

[48] T. K. Haxton, H. Zhou, I. Tamblyn, D. Eom, Z. Hu, J. B. Neaton, T. F. Heinz, and S. Whitelam, *Phys. Rev. Lett*., 2013, **111**, 265701 (1-5).

[49] S. Lee, Z. Yuan, L. Chen, K. S. Mali, K. Müllen, and S. De Feyter, *J. Am. Chem. Soc*., 2014, **136**, 7595−7598.

[50] Y. Wang, H. Xu, H.Wang, S. Li, W. Gan, and Q. Yuan. *RSC Advances* 2014, **4**, 20256–20261.

[51] G. M. Florio, J. E. Klare, M. O. Pasamba, T. L. Werblowsky, M. Hyers, B. J. Berne, M. S. Hybertsen, C. Nuckolls, and G. W. Flynn, *Langmuir*, 2006, **22**, 10003-10008.

[52] K. Kim, K. E. Plass, and A. J. Matzger, *Langmuir*, 2003, **19**, 7149-7152.

[53] A. Stabel, R. Heinz, F. C. De Schryver, and J. P. Rabe, *J. Phys. Chem.*, 1995, **99**, 505-507.

[54] M. J. J. Coenen, M. Cremers, D. den Boer, F. J. van den Bruele, T. Khoury, M. Sintic, M. J. Crossley, W. J. P. van Enckevort, B. L. M. Hendriksen, J. A. A. W. Elemans, and S. Spellera, *Chem. Commun*., 2011, **47**, 9666–9668.

[55] K.W. Hipps, X. Lu, X. D. Wang, and U. Mazur, *J. Phys. Chem*., 1996. **100**, 11207-11210.

[56] X. Lu, K.W. Hipps, X. D. Wang, and U. Mazur, *J. Amer. Chem. Soc.*, 1996, **118,** 7197-7202.

[57] X. Lu and K.W. Hipps, *J Phys. Chem. B*, 1997, **101,** 5391-5396.

[58] L. Scudiero, D. E. Barlow, and K.W. Hipps, *J. Phys. Chem B*, 2000, **104**, 11899-11905.

[59] Q. Ferreira, A.M. Bragan, N.M.M. Moura, M.A.F. Faustino, L. Alcácer, J. Morgado. *Applied Surface Science*, 2013, **273**, 220-225.

[60] D. S. Karpovich and G. J. Blanchard, *Langmuir*, 1994**, 10**, 3315-3322.

[61] M. Alemani, M. V. Peters, S. Hecht, K. Rieder, F. Moresco, L. Grill. *J. Am. Chem. Soc.* 2006, **128**, 14446-14447.

[62] A. Miura, S., De Feyter, M. Abdel-Mottaleb, A. Gesquiére, P. Grim, C. M. Petrus, G. Moessner, M. Sieffert, M. Klapper, K. Müllen, F. C. De Schryver. *Langmuir* 2003, **19**, 6474-6482.

[63] Y. Hasegawa, Ph. Avouris. *Science* 1992, **258**, 1763-1765.

[64] L. Chen, H. Li, A. T. S. Wee. *ACS Nano* 2009, **3**, 3684-3690.

[65] P. Maksymovych, D. B. Dougherty, X.-Y.; Zhu, J. T. Yates. *Phys. Rev. Lett.* 2007, **99**, 016101.

[66] M. Li, D. den Boer, P. Iavicoli, J. Adisoejoso, H. Uji-I, M. Van der Auweraer, D. Amabilino, J. Elemans, S. De Feyter, Steven. *J. Am. Chem. Soc.* **2014, 136**, 17418-17421.

[67] L. Scudiero and K. W. Hipps. *Journal of Physical Chemistry C*, 2007**, 111**, 17516-20.